Chemical Papers (2020) 74:1597–1608
https://doi.org/10.1007/s11696-019-01014-2

ORIGINAL PAPER

Theoretical investigation of the self-association of antitumor drug imexon

Hind Guemmour[1,2] · **Djaffar Kheffache**[1,3]

Received: 2 August 2019 / Accepted: 27 November 2019 / Published online: 4 December 2019

Abstract

The dimers resulting from self-association of oxo-imino, oxo-amino, and hydroxyl-imino tautomers of imexon, that present two hydrogen bonds, were fully optimized with the density functional methods B3LYP, M06-2X in conjunction with 6-311++G(d,p) basis set. Additionally, second-order Møller-Plesset (MP2) level in combination with 6-311++G(d,p) basis set was employed for comparison purpose. The thermodynamic stability of the self assembled structures in gaseous phase has been obtained according to the analyses of total electronic energies and hydrogen bonding interactions. The bulk water environment has been simulated using the universal solvation model based on solute electron density (SMD). Stability and structure of homochiral and heterochiral imexon dimers resulting from the three imexon tautomers have been carried out to investigate the chiral discrimination. The imexon dimer with heterochiral configuration resulting from self-assembling oxo-amino tautomer is found to be thermodynamically most stable in both gas and aqueous phases. The interaction energies for these self assembled structures were further evaluated with the basis set superposition error corrections. The so-called seven-point interaction energy which includes corrections for BSSE and deformation was calculated. The intermolecular interactions of the selected dimers have been analyzed by calculation of electron density (ρ) and Laplacian ($\nabla^2\rho$) at the bond critical points (BCPs) using atoms-in-molecule (AIM) theory.

Keywords Imexon · Self-association · Hydrogen bond · DFT · AIM method

Introduction

Imexon (4-imino-1,3-diazabicyclo[3,1,0]-hexan-2-one) is a member of the class of 2-cyanoaziridine derivatives, which has been of interest as immunomodulators and promising anticancer agents (Remers and Dorr 2012; Sheveleva et al. 2012; Moulder et al. 2010). One of the more important characteristics of imexon is that it may exist in three different tautomeric forms (Remers and Dorr 2012), namely oxo-imino (Imex1), oxo-amino (Imex2), and hydroxyl-imino (Imex3), as illustrated in Fig. 1. Previously, we have investigated in detail the prototropic tautomerism and microsolvation in antitumor drug imexon using density functional theory (DFT) (Kheffache et al. 2010, 2012). It emerges from this study that in gas phase, the most stable tautomer corresponds to oxo-imino (Imex**1**) structure, whereas in aqueous solution the oxo-amino (Imex**2**) tautomer was found to be the most predominant form (Kheffache and Ouamerali 2010; Kheffache et al. 2012). We have also found that oxo-imino (Imex1) and oxo-amino tautomers are nearly equivalent in energy. Additionally, one of the most significant findings in our previous study (Kheffache et al. 2012) was the catalytic effect of water molecules in the tautomerism of imexon. Indeed, microhydration with one and two solvating water molecules considerably lowers the tautomerism activation barriers for proton transfer. Furthermore, the NMR

Electronic supplementary material The online version of this article (https://doi.org/10.1007/s11696-019-01014-2) contains supplementary material, which is available to authorized users.

✉ Hind Guemmour
hguemmour@yahoo.fr

[1] Chemistry Department of the Faculty of Sciences, University M'Hamed Bougara (UMBB), 35000 Boumerdes, Algeria

[2] Laboratory of Macromolecular Synthesis and Thio-organic Macromolecular, Faculty of Chemistry, University of Sciences and Technology Houari Boumediene (USTHB), BP 32, El Alia, 16000 Algiers, Algeria

[3] Laboratory of Computational Chemistry and Photonics, Faculty of Chemistry, University of Sciences and Technology Houari Boumediene (USTHB), BP 32, El Alia, 16000 Algiers, Algeria

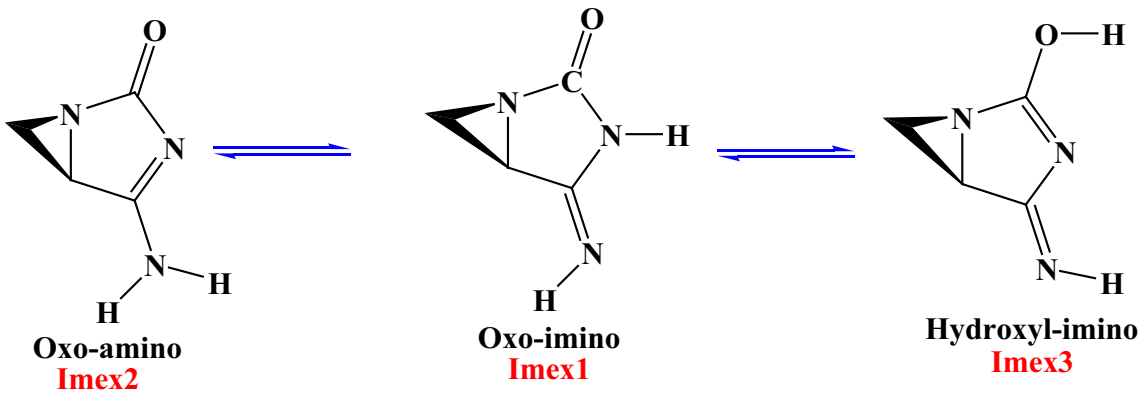

Fig. 1 Schematic representation of the most stable tautomers/rotamers of imexon (Kheffache et al. 2012; Den Brok et al. 2005) Adopted nomenclature for tautomers is presented

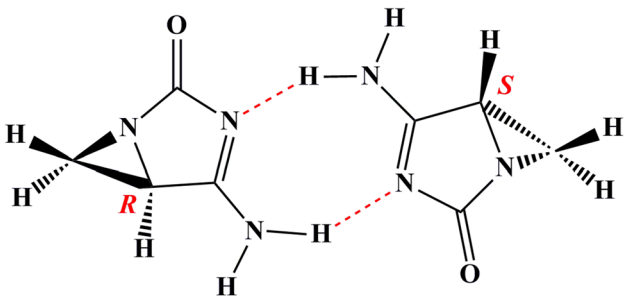

Fig. 2 Schematic representation of the structure of imexon in solid state (Kuehl et al. 2006). The dimer presents heterochiral configuration (RS)

observation (Den Brok et al. 2005) compared with our DFT calculation of ^{1}H and ^{13}C chemical shifts (Kheffache and Ouamerali 2010) strongly suggests the existence of imexon in its oxo-amino (Imex**2**) tautomeric system in solution.

There is no analysis of the structure of imexon in solution, but an X-ray diffraction study reported by Kuehl et al. (2006) indicated that the crystal structure of imexon adopts hydrogen-bonded dimeric units which is linked through intermolecular hydrogen bonds into continuous tapes of pairs of molecules, as illustrated in Fig. 2.

The tautomers of imexon (Fig. 1) offer the possibility of formation of intermolecular hydrogen bonds of different types: NH····O, NH····N, and OH····N. Consequently, we might expect the formation of different kinds of imexon dimeric self-association in gas and solution phases. It is worth mentioning that the tendency for self-association, that may have the antitumor drug imexon, can potentially impact its cellular bioavailability and activity.

Based on the above, the study of self-association of anti-cancer agent imexon is an important problem. To the best of our knowledge, in spite of a number studies on imexon, there are no theoretical studies relating to the relative stabilities of self-association of imexon tautomers. Hence, in the present work, ab initio and DFT calculations were carried out to give deeper insight into the nature of forces governing the self-association of imexon monomeric units, essential for a better physicochemical description of parent drug. The imexon dimeric structures taken into consideration in this investigation are those resulting from self-assembling oxo-imino, oxo-amino, and hydroxyl-imino tautomers. Only those configurations with simultaneous double hydrogen bonds have been explored. The effect of solvation has been taken into account using the universal solvation model based on solute electron density (SMD) (Marenich et al. 2009).

As a result of the presence of one chiral center at the bridge head carbon atom of imexon (see Fig. 1) for each dimer, two complexes that differ in energy could be formed: the homochiral (*RR* or *SS*) and the heterochiral (*RS* or *SR*) structures. Chiral discrimination through hydrogen-bonded compounds is of great importance, because compounds with opposite chirality can have different biological activities (Alkorta et al. 2006a, b). The degree of chiral discrimination corresponds to the difference in energy between the homochiral dimers (*RR* or *SS*) and the analogous heterochiral dimers (*RS* or *SR*).We addressed this question here by examining the chiral discrimination resulting from the homochiral (*RR*) and heterochiral (*RS*) self-association of the three imexon tautomers. According to X-ray diffraction data (Kuehl et al. 2006), crystal structure of imexon shows a self-association of oxo-amino tautomer with heterochiral configuration (RS) (Fig. 2).

The present work concerns a careful study of self-association of imexon tautomers to explore the geometries, relative energies, interaction energies, and intermolecular interactions of all potential dimers of imexon. We hope that this investigation may provide some valuable information on self-association behavior of imexon and could provide

a valuable guide for developing the chemistry of antitumor drug imexon.

Computational methods

The geometry optimization of all dimers reported in the present work was performed with the hybrid Becke three parameter Lee–Yang–Parr DFT-B3LYP (Becke 1993; Lee et al. 1988) and meta-hybrid functional M06-2X developed (Zhao and Truhlar 2008) in conjunction with the 6-311++G (d,p) basis set. Further characterization of the stationary points was performed using second-order Møller-Plesset (MP2) (Møller and Plesset 1934) along with 6-311++G(d,p) basis set.

All of the theoretical calculations reported in this investigation were carried out using the Gaussian 16 suite of program (Frisch et al. 2016). Harmonic vibrational frequencies were evaluated at different levels to confirm the nature of the stationary points found and also to account for the zero-point vibrational energy (ZPVE) correction.

To simulate the effect of water bulk solvation, a single-point SMD (solvation model based on density) calculation (Marenich et al. 2009) was performed on the optimized structures.

The uncorrected interaction energy expressed as the difference in electronic energies of the monomers and the dimer is given by the following:

$$\Delta E_{\text{int}} = E_{AA'} - E_A^A - E_{A'}^{A'}. \tag{1}$$

The interaction energy corrected for the zero-point vibrational energy (ZPVE) of the monomers and the dimer is given by:

$$\Delta \text{E}_{\text{int}}^{\text{ZPVE}} = E_{AA'}(\text{ZPVE}) - E_A^A(\text{ZPVE}) - E_{A'}^{A'}(\text{ZPVE}). \tag{2}$$

The interaction energy corrected for the inherent basis set superposition error (BSSE) using the full counterpoise method as proposed by Boys and Bernardi (1970) was calculated according to:

$$\Delta E_{\text{CP}} = E_{AA'} - E_{A.\text{def}}^{AA'} - E_{A'.\text{def}}^{AA'}. \tag{3}$$

The $\Delta E_{int}^{\text{ZPVE/BSSE}}$ interaction energy (Eq. 4) consist both zero-point vibrational energy (ZPVE) and BSSE correction Eq. (4):

$$\Delta E_{\text{int}}^{\text{ZPVE/BSSE}} = \Delta \text{E}_{\text{int}}^{\text{ZPVE}} + \text{BSSE}. \tag{4}$$

Finally, the so-called seven-point interaction energy (Rode and Dobrowolski 2002; Rode et al. 2012), ΔE_7, was calculated, which includes corrections for BSSE and deformation energy as:

$$\Delta E_7 = E_{AA'} - E_A^A - E_{A'}^{A'} - E_{A.\text{def}}^{AA'} - E_{A'.\text{def}}^{AA'} + E_{A.\text{def}}^{A} + E_{A'.\text{def}}^{A'}. \tag{5}$$

The deformation energy $\left(\Delta E_{\text{def}}\right)$ is determined as:

$$\Delta E_{def} = \Delta E_7 - \Delta E_{CP} = E_{A.def}^{A} + E_{A'.def}^{A'} - E_A^A - E_{A'}^{A'}, \tag{6}$$

where $E_{AA'}$ denotes the energy of dimer, E_A^A and $E_{A'}^{A'}$ represent the energies of dimer components optimized in their own basis set. $E_{A.\text{def}}^{AA'}$ and $E_{A'.\text{def}}^{AA'}$ denote the energies of monomers with geometries taken from dimer in basis set of dimer. $E_{A.\text{def}}^{A}$ and $E_{A'.\text{def}}^{A'}$ denote the energies of monomers with geometries taken from self-associated dimer treated with their own basis sets.

To evaluate the nature of hydrogen bonding interactions in imexon dimers, the electron density of the systems has been analyzed by the atoms-in-molecules (AIM) methodology (Bader 1985; Carroll and Bader 1988) using the Multiwfn program (Lu and Chen 2012) at the M06-2X/6-311++G(d,p) level. It is well known that the relative strength of bond could be obtained in terms of electron density (ρ), and Laplacian ($\nabla^2\rho$) (Koch and Popelier 1995; Popelier 1998; Matta and Boyd 2007).

The free energy of association in aqueous phase has been calculated using the following relationship:

$$\Delta G_{\text{ass}}^{*} = G_{\text{dimer}}^{*} - 2G_{\text{monomer}}^{*},$$

where G_{dimer}^{*} and G_{monomer}^{*} are the total Gibbs free energies of the dimer and monomer in aqueous solution at 298 K.

The value of G^* in aqueous solution was determined as the sum of the following terms:

$$G^{*} = G^{0} + \Delta G_{\text{solv}} + \Delta G^{0\rightarrow *},$$

where G^0 is the thermal free energy in gas phase, ΔG_{solv} is solvation free energy of the solute, and $\Delta G^{0\rightarrow *}$ =1.89 kcal mol^{-1} (T=298.15 K) is the correction for changing the standard state from gas phase (1 atm) to solution (1 mol L^{-1}) (Ribeiro et al. 2011).

Results and discussion

Relative energies

We begin by examining the relative stability of the different dimers resulting from self-association of the three tautomeric forms of imexon (Kheffache et al. 2012; Den Brok et al. 2005) (oxo-imino, oxo-amino, and hydroxyl-imino) in vacuum and in water solution. It should be noted that only dimers with two hydrogen bonds have been considered since they are more stable than the dimers with only one hydrogen bond. Notice that the self-association of the three imexon tautomers gives for each complex two

possible configurations, the homochiral (*RR* or *SS*) and heterochiral (*RS* or *SR*) configurations as illustrated in Fig. 3, where we report also the numbering scheme and the nomenclature used in this paper.

All dimers were fully optimized without any constraints; the optimizations were performed in the gas phase using the B3LYP, M06-2X in conjunction with the 6-311++G(d,p) basis set. The energies were also calculated using the accurate MP2/6-311++G(d,p) level for comparison purpose.

The relative energies with ZPVE correction ($\Delta E_{(ZPVE)}$) obtained in gas phase for the most stable imexon dimers (homo and heterochiral) are collected in Table 1, Table S1 of Supplementary Materials for all dimers considered in this study. More details on absolute energies can also be found in Table S2.

The presented data permit to conclude that the 2Imex**2**-(*RS*) dimer resulting from self-association of oxo-amino tautomer (Imex**2**) is thermodynamically the most stable under gas phase condition. Interestingly, the relative stabilities of the dimers are not similar to those of the monomeric units (Kheffache et al. 2012; Kheffache and Ouamerali 2010). Indeed, the oxo-imino (Imex**1**) tautomer was found to be the most stable structure in gas phase (Kheffache et al. 2012; Kheffache and Ouamerali 2010), whereas self-association leads to the stabilization of the dimer (2Imex**2**-(*RS*)) resulting from oxo-amino monomer (Imex**2**). Our prediction that 2Imex**2**-(*RS*) is the most stabilized dimer is in interesting agreement with the reported X-ray structure of imexon (Kuehl et al. 2006).

From Table S1, one can see that all dimers resulting from self-association of oxo-imino (Imex**1**) tautomer are relatively less stable; the formation of these dimers is thermodynamically quite feasible.

Comparison of $\Delta E_{(ZPVE)}$ values given in Table 1 shows that the relative energy difference between 2Imex**1b**-(*RS*)/-(*RR*) dimers and 2Imex**2**-(*RS*) is very low value. The maximum relative energy ($\Delta E_{(ZPVE)}$) between these dimers is obtained at M06-2X level ($\Delta E_{(ZPVE)} = 1.49$ kcal mol^{-1}), while MP2/6-311++G(d,p) level gives a corrected relative energy of 0.97 kcal mol^{-1}. Hence, a substantial amount of 2Imex**1b**-(*RS*)/-(*RR*) and 2Imex**2**-(*RS*)/-(*RR*) may be present in gas phase. It must be further mentioned that in gas phase, all dimers resulting from self-association of hydroxyl-imino tautomer (Imex**3**) are remarkably less stable and these structures cannot be expected in gas phase or in solid-state conditions.

The sequence of relative stability of the studied dimers obtained at different levels (Table S1, supplementary materials) can be written in the following order: 2Imex**2**-(*RS*)/-(*RR*) > 2Imex**1b**-(*RS*)/-(*RR*) >> 2Imex**1c**-(*RS*)/-(*RR*) > 2Imex**1a**-(*RS*)/-(*RR*) >>> 2Imex**3a**-(*RS*)/-(*RR*) -> 2Imex**3c**-(*RS*)/-(*RR*) > 2Imex**3b**-(*RS*)/-(*RR*).

The biological activity of a drug is usually tested in an aqueous solution, rather than in gas phase and the stability of the dimers may also differ from the form they adopt in the isolated state. To study the relative stability of the above dimers in aqueous medium, we considered the solvation effect using the solvation model density (SMD) continuum solvation model on the optimized geometry obtained in gas phase.

The solvent effect is given in Table 2, where the relative electronic energies obtained for the most stable imexon dimers at different levels in aqueous solution are presented (more details on absolute electronic energies and relative energies are listed on Tables S3–S4 of the supplementary materials).

The results which were collected in Table 2 (in Table S3 of Supplementary Materials for of all dimers) lead to the conclusion that the solvent has no impact on the dimers' stability. This result reveals the great stabilization of dimeric self-association of the oxo-amino tautomer 2Imex**2**-(*RS*)/-(*RR*), in aqueous solution. The estimation of the ΔG_{solv} in water, using the SMD solvation model, is listed in Table 2 (in Table S3 of Supplementary Materials for of all dimers). The solvation free energies ΔG_{solv} show clearly that 2Imex**2**-(*RS*)/-(*RR*)) are the most solvated dimers which should increase their population in solution.

Chiral discrimination

The chiral discrimination in the formation of hydrogen-bonded (HB) dimers of imexon tautomers was studied by means of B3LYP, M06-2X, and MP2 calculations.

Table 3 shows the chiral discrimination E^{Chir}_{ZPVE} values obtained, for each dimer, as the difference between the homochiral and the heterochiral configurations, using the following equation:

$$E^{Chir}_{ZPVE} = E^{RS}_{dimer(ZPVE)} - E^{RR}_{dimer(ZPVE)}.$$

Homochiral dimer is used as reference in all cases. $E^{RS}_{dimer(ZPVE)}$ and $E^{RR}_{dimer(ZPVE)}$ are the sum of electronic and zero-point energies of homochiral and heterochiral configurations of the dimer.

The three theoretical levels considered here provide very similar results with the same sign for chiral discrimination $\left(E^{Chir}_{ZPVE}\right)$ in gas phase. The results shown in Table 3 clearly demonstrate that, in all cases, the heterochiral self-association (RS or SR) is preferred over the homochiral one (RR or SS). The very small chiral discrimination found in the studied dimers could be due to the fact that the asymmetric carbon atoms C_3 and $C_{3'}$ (Fig. 3) are distant from the interaction area.

The solvent effect on chiral discrimination has also been studied. From Table 3, we can see that low chirality

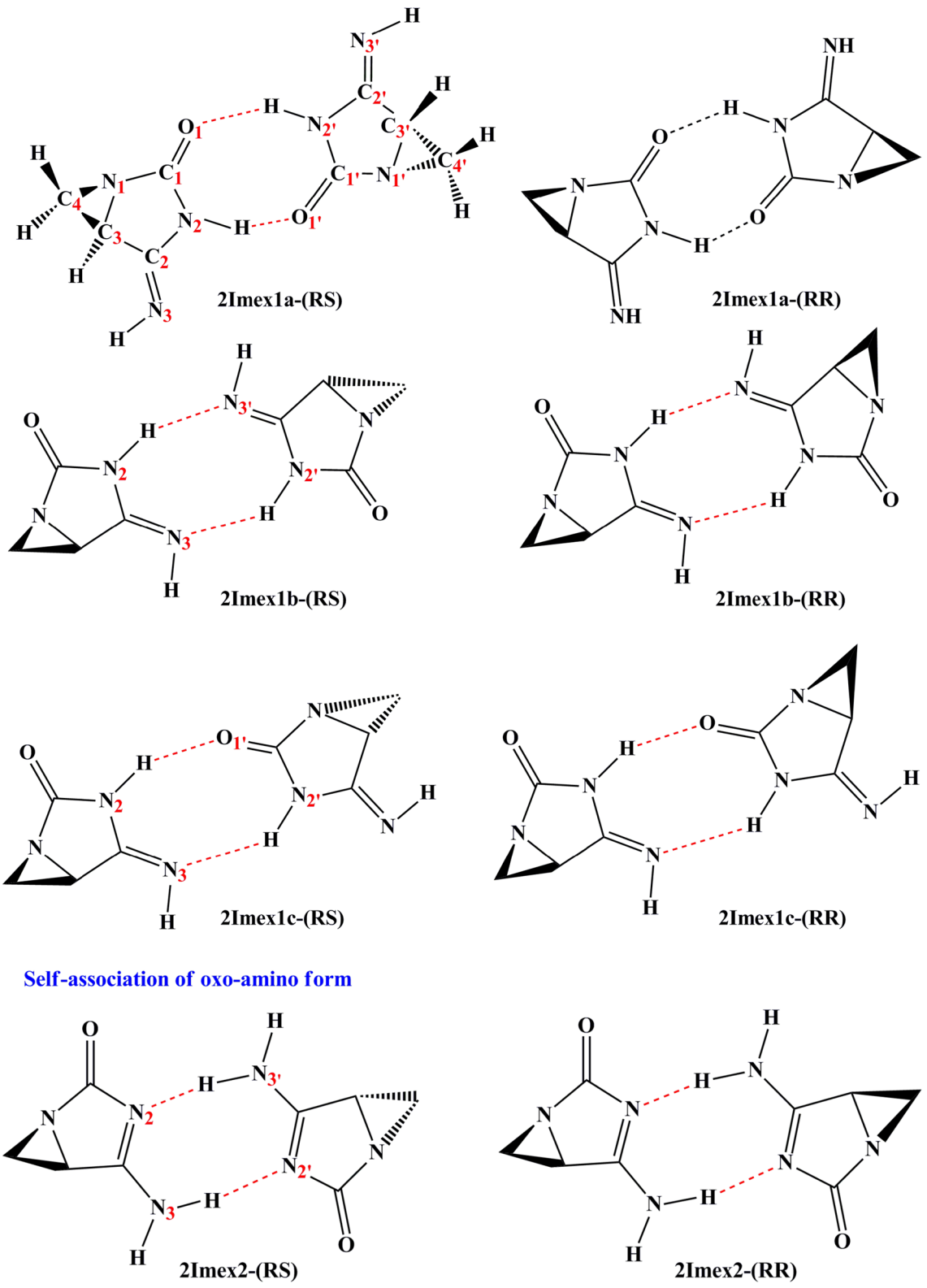

Fig. 3 Schematic representation of the homochiral and heterochiral self-association dimers of imexon. Standard numbering and adopted nomenclature for dimers are presented

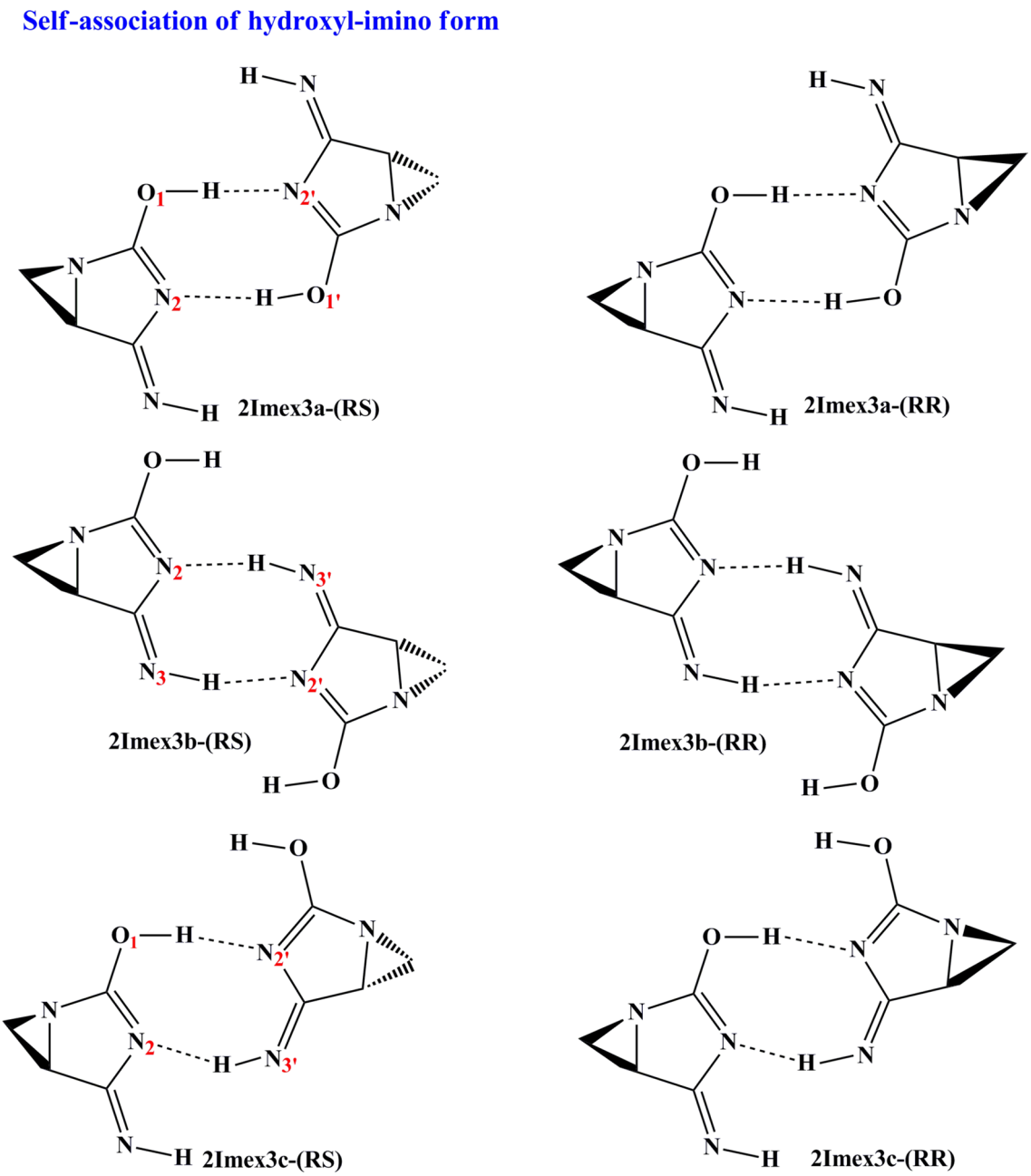

Fig. 3 (continued)

Table 1 Zero-point corrected relative energies $\Delta E_{(ZPVE)}$ (kcal mol^{-1}) and dipole moment μ (Debye) of the most stable self-association dimers in gas phase at different levels employing 6-311++G(d,p) basis set

Species	B3LYP		M06-2X		MP2	
	$\Delta E_{(ZPVE)}$	μ	$\Delta E_{(ZPVE)}$	μ	$\Delta E_{(ZPVE)}$	μ
2Imex**1b**-(RR)	1.49	3.09	1.49	3.19	0.97	3.71
2Imex**1b**-(RS)	1.44	0.00	1.47	0.00	0.69	0.00
2Imex**2**-(RR)	0.03	2.42	0.05	2.41	0.002	2.55
2Imex**2**-(RS)	0.00	0.00	0.00	0.00	0.00	0.00

Table 2 Relative energy ΔE_0 (kcal mol^{-1}), solvation free energy ΔGs (kcal mol^{-1}) and dipole moment μ (Debye) of the most stable self-association dimers in water solution obtained using SMD model of solvation

Species	B3LYP			M06-2X			MP2		
	ΔE_0	ΔGs	μ	ΔE_0	ΔGs	μ	ΔE_0	ΔGs	μ
2Imex**1b**-(RR)	5.85	−30.73	4.39	5.78	−30.73	4.499	4.04	−22.89	4.79
2Imex**1b**-(RS)	5.89	−30.59	0.00	5.83	−30.59	0.00	4.19	−22.82	0.00
2Imex**2**-(RR)	0	−35.89	3.46	0	−35.80	3.39	0	−26.41	3.14
2Imex**2**-(RS)	0.001	−35.90	0.00	0.01	−35.89	0.00	0.09	−26.25	0.00

Used basis set is 6-311++G(d,p)

Table 3 ZPVE corrected chiral discrimination E^{Chir}_{ZPVE} (kJ mol^{-1}) in gas phase and chiral discrimination E^{Chir}_0 (kJ mol^{-1}) in aqueous solution calculated using different levels in combination with 6-311++G(d,p) basis set

Dimer (RS)/-(RR)	Gas phase			Aqueous phase		
	B3LYP	M06-2X	MP2	B3LYP	M06-2X	MP2
	E^{Chir}_{ZPVE}	E^{Chir}_{ZPVE}	E^{Chir}_{ZPVE}	E^{Chir}_0	E^{Chir}_0	E^{Chir}_0
2Imex**1a**-(RS)/-(RR)	−0.88	−1.17	−1.48	−0.52	−0.33	−0.35
2Imex**1b**-(RS)/-(RR)	−0.83	−0.43	−4.96	0.72	0.96	−1.19
2Imex**1c**-(RS)/-(RR)	−1.59	−1.70	−1.18	−0.47	−0.39	−0.28
2Imex**2**-(RS)/-(RR)	−0.68	−0.99	−0.04	0.03	0.19	−0.01
2Imex**3a**-(RS)/-(RR)	−1.60	−2.43	−1.23	0.21	0.73	−0.29
2Imex**3b**-(RS)/-(RR)	−0.49	−1.38	−0.50	1.83	1.85	−0.12
2Imex**3c**-(RS)/-(RR)	−0.89	−0.85	−0.15	0.45	0.50	−0.04

The homochiral dimer is used as reference in all cases

Table 4 Optimized hydrogen bonds of selected imexon self-association heterochiral dimers obtained at B3LYP and M06-2X employing 6-311+G(d,p) basis set, bond lengths (Å), and bond angles (°) in the A–H·····B H-bond

Dimers	$d_{A–H}$	$d_{B\cdots H}$	$d_{A\cdots B}$	<A–H·····B
2Imex1b-(RS)				
N–H·····N	1.038[a]	1.879	2.905	169.1
	1.035[b]	1.874	2.897	168.8
2Imex2-(RS)				
N–H·····N	1.037 (0.880) [c]	1.871 (2.010)	2.897 (2.881)	169.3 (172.0)
	1.034	1.864	2.881	167.1
2Imex3a-(RS)				
O–H·····N	1.052	1.543	2.595	178.2
	1.063	1.491	2.555	177.7

a B3LYP/6-311++G(d,p)

b M06-2X/6-311+G(d,p)

c X-ray parameters (Kuehl et al. 2006) are given in parentheses

discrimination has also been observed in water solution. In several cases, the homochiral configurations (RR or SS) became the preferred configuration, in contrast with the gas phase results.

Intermolecular hydrogen bonds

Table 4 gives the values of distances and angles for intermolecular A–H·····B hydrogen bond from the experiment (Kuehl et al. 2006) and theoretical calculation obtained for heterochiral dimers 2Imex**1b**-(*RS*), 2Imex**2**-(*RS*), and 2Imex**3a**-(*RS*).

The H-bond parameters obtained from our calculations indicate that the interactions between two identical tautomers of imexon produce symmetric cyclic dimers. Let us remember that the 2Imex**2**-(*RS*) dimer resulting from self-association of the oxo-amino tautomer is topologically similar to the structure observed in solid state (Kuehl et al. 2006). For 2Imex**2**-(*RS*), our calculations deliver NH····N (H····N_2 and H····$N_{2'}$) distance of 1.871Å at B3LYP/6-311++(d,p) and 1.864 Å at M06-2X/6-311++(d,p), which are shorter than those of X-ray values (2.010 Å). Considering the low accuracy of the X-ray analysis in determining the H positions, the value of the experimental NH····N distance should be considered with caution. More accurate confrontation of the experimental to the theoretical hydrogen bond is possible by investigating the N·····N distance (N_2·····$N_{3'}$ and N_3·····$N_{2'}$) of 2Imex**2**-(*RS*) dimer. Inspection of the results reported in Table 3 shows that M06-2X/6-311++(d,p) gives identical hydrogen bond distance 2.881 Å for N_2·····$N_{3'}$ and N_3·····$N_{2'}$, which is in very good agreement with the experimental value 2.881 Å (Kuehl et al. 2006).

The arrangement of atoms, hydrogen bond participants has been established by X-ray analysis to be about linear ($<N_2–H\cdots N_{3'}=<N_3–H_1\cdots N_{2'}=172°$). According to B3LYP and M06-2X levels, these hydrogen bond angles are 169.3° and 167.1°, respectively, which are in acceptable agreement with the experimental value.

The data reported in Table 4 indicate also that dimers resulting from self-association of Imex**1** monomer are hydrogen-bonded clusters. The formation of two symmetrical intermolecular H-bonds NH····N=C is favored in 2Imex**1b**-(*RS*) structure. Our calculation delivers NH····N=C (H····N_3 and H····$N_{3'}$) distance of 1.038 Å at B3LYP/6-311++G(d,p) and 1.035 at M06-2X/6-311++G(d,p).The calculated $<N_{3'}\cdots H–N_2$ and $<N_3\cdots H–N_{2'}$ angles of 169.1° with B3LYP level and 168.8° at M06-2X level is the result of an almost linear hydrogen bond.

As can be seen in Table 4, the dimer 2Imex**3a**-(*RS*) possesses two strong hydrogen bonds O–H····N (H····N_2 and H····$N_{2'}$) with length of 1.543Å at B3LYP/6-311++(d,p). Note also that $<N_2\cdots H–O_{1'}$ and $<N_{2'}\cdots H–O_1$ angles are 178.2°, showing a practically linear arrangement and very strong interaction.

More strict evaluation of the intermolecular hydrogen bonds in the dimers will be presented below on the basis of the calculated hydrogen-bonded interaction energies and AIM analysis.

Interaction energies

The interaction energies (ΔE_{CP}) corrected for the BSSE by Boys–Bernardi counterpoise method, the ZPVE/BSSE-corrected interaction energies $(\Delta E_{int}^{ZPVE/BSSE})$ and interaction energies corrected for BSSE by seven-point method (ΔE_7) calculated by means of B3LYP, M06-2X, and MP2 are listed in Table 5. The interaction energies ΔE_{int}^{ZPVE}, the basis set superposition error (BSSE) and deformation energies (ΔE_{def}) are listed in Table S5, which is available as supplementary data.

From Table S5, it can be seen that the effect of the BSSE correction calculated at DFT levels is not very significant. On the other hand, the BSSE correction at the MP2 level is much higher. It is therefore necessary to check the BSSE correction at MP2 level.

It should be noted that the incorporation of BSSE correction brings down the values of interaction energy $(\Delta E_{int}^{ZPVE/BSSE})$, but does not modify the sequence provided by ΔE_{int}^{ZPVE} at both DFT and MP2 levels. The $\Delta E_{int}^{ZPVE/BSSE}$ obtained for the most favorable dimer 2Imex2-(*RS*) is − 17.77 kcal mol^{-1} at B3LYP, − 19.46 kcal mol^{-1} at M06-2X, and − 18.00 kcal mol^{-1} at MP2 level of theory. The dimers resulting from self-association of Imex1 monomer also possess fairly large interaction energy $(\Delta E_{int}^{ZPVE/BSSE})$ and are in the range of − 10 and − 14 kcal mol^{-1} (Table 5).

Upon examination of Table 5, the use of Boys–Bernardi counterpoise procedure leads to a large description of the

Table 5 Interaction energies corrected for the BSSE by Boys–Bernardi counterpoise method ΔE_{CP}, ZPVE/BSSE-corrected interaction energies ($\Delta E_{int}^{ZPVE/BSSE}$), interaction energies corrected for the BSSE by seven-point method ΔE_7

Dimers	B3LYP/6-311++G(d,p)			M06-2X/6-311++G(d,p)			MP2/6-311++G(d,p)		
	ΔE_{CP}	$\Delta E_{int}^{ZPVE/BSSE}$	ΔE_7	ΔE_{CP}	$\Delta E_{int}^{ZPVE/BSSE}$	ΔE_7	ΔE_{CP}	$\Delta E_{int}^{ZPVE/BSSE}$	ΔE_7
2Imex**1a**-(RR)	− 15.21	− 10.59	− 11.6	− 16.42	− 11.99	− 12.85	− 14.39	− 10.36	− 11.11
2Imex**1a**-(RS)	− 15.29	− 10.64	− 11.66	− 16.47	− 12.04	− 12.91	− 14.43	− 10.45	− 11.15
2Imex**1b**-(RR)	− 15.40	− 13.03	− 13.99	− 16.57	− 14.57	− 15.29	− 15.46	− 13.67	− 14.42
2Imex**1b**-(RS)	− 15.43	− 13.06	− 14.04	− 16.61	− 14.58	− 15.34	− 15.51	− 13.94	− 14.47
2Imex**1c**-(RR)	− 13.15	− 10.99	− 11.97	− 14.39	− 12.47	− 13.3	− 13.05	− 11.46	− 12.18
2Imex**1c**-(RS)	− 13.24	− 11.07	− 12.07	− 14.49	− 12.55	− 13.4	− 13.16	− 11.5	− 12.28
2Imex**2**-(RR)	− 21.21	− 17.73	− 19.38	− 22.69	− 19.40	− 20.9	− 20.63	− 17.99	− 18.87
2Imex**2**-(RS)	− 21.27	− 17.77	− 19.43	− 22.73	− 19.46	− 20.94	− 20.68	− 18.00	− 18.96
2Imex**3a**-(RR)	− 31.58	− 22.84	− 22.29	− 35.33	− 25.17	− 24.18	− 25.13	− 20.70	− 20.53
2Imex**3a**-(RS)	− 31.70	− 22.93	− 22.38	− 35.49	− 25.31	− 24.26	− 25.22	− 20.78	− 20.61
2Imex**3b**-(RR)	− 4.41	− 3.52	− 4.32	− 6.13	− 5.29	− 6.02	− 5.99	− 5.31	− 5.91
2Imex**3b**-(RS)	− 4.44	− 3.55	− 4.35	− 6.24	− 5.36	− 6.13	− 6.01	− 5.34	− 5.93
2Imex**3c**-(RR)	− 12.56	− 10.25	− 10.97	− 14.38	− 12.28	− 12.84	− 12.42	− 10.8	− 11.4
2Imex**3c**-(RS)	− 12.61	− 10.3	− 11.03	− 14.43	− 12.33	− 12.9	− 12.45	− 10.83	− 11.43

All values are in kcal mol^{-1}

ΔE_{CP} interaction energy corrected for BSSE in the counterpoise method

$\Delta E_{int}^{ZPVE/BSSE}$ interaction energy corrected for ZPVE and BSSE

ΔE_7 interaction energy corrected for BSSE and deformation

interaction energy (ΔE_{CP}), probably due to the large destabilizing contribution of the structural deformation energy (ΔE_{def}). For this reason, the seven-point method ΔE_7, which includes both counterpoise correction and deformation energy of the dimer components that have been calculated and listed in Table 5. The introduction of seven-point method makes the interaction energy ΔE_7 smaller in absolute value, but do not change the energy order of the studied dimers (Table 5). The most stable dimer was found to have an interaction energy ΔE_7 of − 18.96 kcal.mol^{-1} at MP2/6-311++G(d,p).

What is however remarkable is that, in all cases, the interaction energies of self-associated dimers 2Imex3a-(*RS*)/-(*RR*) are the most negative (see Table 5). The higher interaction energy observed for 2Imex3a (*RS*)/-(*RR*) indicates a strong O–H···N hydrogen bond interaction between the two Imex3 monomers. It may be of some interest to remark that the interaction energy, in magnitude, do not correlate with the thermodynamic stability order of the dimers.

It is also worth noticing that the deformation energy of 2Imex2-(*RS*)/-(*RR*) dimers is less than 2 kcal/mol, indicating that the monomer geometries change little upon dimers formation.

Focusing on the 2Imex1a (*RS*)/-(*RR*) and 2Imex3a (*RS*)/-(*RR*) dimers, it was observed that the deformation energies (ΔE_{def}) are more significant.

AIM electron density at bond critical points

To obtain additional information about the strengths of intermolecular hydrogen bonds in the selected imexon dimers 2Imex1b-(*RS*), 2Imex**2**-(*RS*), and 2Imex**3a**-(*RS*), we carried out AIM analysis of the electron density at bond critical points (Matta and Boyd 2007) using the wave functions obtained at M06-2X/6-311++G(d, p) level of theory. It was shown that Laplacian value of the electron density, as well as electron density in bond and ring critical points of the hydrogen bonds correlate with hydrogen bond strength (Koch and Popelier 1995; Matta and Boyd 2007). According to AIM methodology, the hydrogen bonds (HB) are characterized by the presence of a bond critical points (BCPs) associated with a bond path between an HB acceptor (oxygen, nitrogen) and the hydrogen atom of the HB donor moiety (hydroxyl and amino groups) (Koch and Popelier 1995; Popelier 1998).The values of the electron density (ρ) and its Laplacian ($\nabla^2\rho$) at these critical points give valuable information about the strength of the hydrogen bonds. Two quantitative criteria have been suggested by (Koch and Popelier 1995; Popelier 1998) to characterize the strength of a hydrogen bond: the electron density (ρ) should be within the range 0.002–0.040 a.u and its Laplacian ($\nabla^2\rho$) should be within the range 0.024–0.139 a.u.

The topological parameters such as electron density $\rho(r)$, Laplacian of electron density $\nabla^2\rho(r)$, potential energy density $V(r)$, Lagrangian kinetic energy $G(r)$, and Hamiltonian kinetic energy $H(r)$ at H-bond critical points (BCPs) of the three selected imexon dimers 2Imex1b-(*RS*), 2Imex**2**-(*RS*), and 2Imex3a-(*RS*) are collected in Table 6. The energy of the different hydrogen bonds has been calculated using the relationship $E_{HB} = V(r)/2$ described by (Espinosa et al. 1998), in which $V(r)$ is the potential energy density at H-bond critical points (BCPs). Figure 4 also displays the molecular graphs of the selected imexon dimers: 2Imex1b-(*RS*), 2Imex**2**-(*RS*), and 2Imex3a-(*RS*).

As shown in Table 6, the calculated density $\rho(r)$ and Laplacian $\nabla^2\rho(r)$ for BCPs at the different hydrogen bonds are obtained identical for each of the three dimers 2Imex1b-(*RS*), 2Imex**2**-(*RS*), and 2Imex3a-(*RS*), the H-Bonds were then found symmetrical.

In the case of N····HN interaction (N_2·····HN_3, and N_2,····HN_3) present in the most stable dimer 2Imex**2**-(*RS*), the electron density $\rho(r)$ is 0.0352 a.u, and its Laplacian $\nabla^2\rho(r)$ is 0.0996 a.u (see Table 6 and Fig. 4) fulfilling the topological criteria proposed by Koch and Popelier (Koch and Popelier 1995; Popelier 1998) for hydrogen bond.

Table 6 Topological parameters for hydrogen bonded interactions

Dimers	$\rho(r)$	$\nabla^2\rho(r)$	$V(r)$	$G(r)$	$H(r)$	$-G(r)/V(r)$	$E_{HB} = V(r)/2$
2Imex**1**-**b**-(RS)							
N_3·····HN_2, N_3,·····HN_2	0.0344	0.0966	− 0.0272	0.0257	− 0.0015	0.9448	− 8.53
2Imex**2**-(RS)							
N_2·····HN_3, N_2,····H N_3	0.0352	0.0996	− 0.0283	0.0266	− 0.0017	0.9399	− 8.88
2Imex**3**-**a**-(RS)							
N_2····HO_1, N_2,····HO_1	0.0887	0.0653	− 0.0943	0.0553	− 0.0390	0.5864	− 29.58

Electron density $\rho(r)$, Laplacian of electron density $\nabla^2\rho(r)$, potential energy density V(r), Lagrangian kinetic energy $G(r)$, Hamiltonian kinetic energy $H(r)$ and H-bond energy E_{HB} at the M06-2X/6-311+G(d,p) calculation. All quantities are in atomic unit (a.u.) except E_{HB} (kcal mol^{-1})

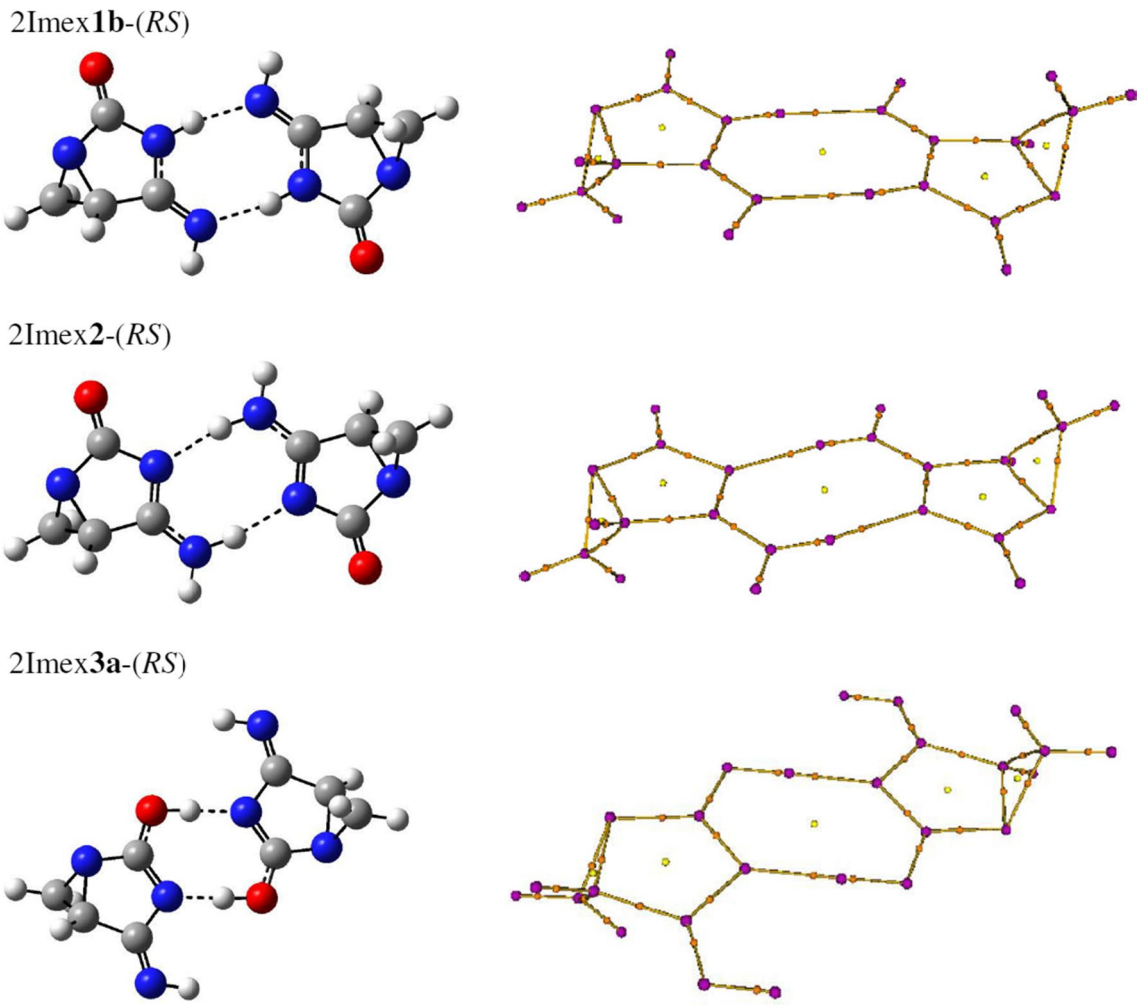

Fig. 4 The optimized geometries (left) and the molecular graphs (right) for dimers at M06-2X/6-311 + G(d,p). Small red spheres, small yellow spheres, and lines correspond to the bond critical points (BCP), ring critical points (RCP), and bond paths, respectively as calculated using Multiwfn program

In the case of 2Imex1b-(*RS*) dimer, the $\rho(r)$ and $\nabla^2\rho(r)$ of BCPs at N····NH interactions (N_3·····HN_2, and N_3,····HN_2) are 0.0344 and 0.0966 a.u respectively, thus confirming the formation of N····NH H-bonds in 2Imex1b-(*RS*) dimer.

The values of $\rho(r)$ (0.0887 a.u) and $\nabla^2\rho(r)$ (0.0653 a.u) of BCPs at O–H····N interactions (2Imex3a-(*RS*)) are within the common accepted values for H-bonding interactions. It is to be noted that higher electron density $\rho(r)$ (0.0887 u.a) has been obtained for the O–H····N interactions of 2Imex3a-(*RS*) dimer than the one calculated for N····HN interactions ($\rho(r) = 0.0352$ u.a) present in the most stable dimer 2Imex**2**-(*RS*). The relatively high value of the charge density at BCP of O–H····N (O_1,H····N_2 and O_1H····N_2) is a characteristic of strong hydrogen bonding, which is also consistent with the above given H-bond geometrical characterization.

The ratio $-G(r)/V(r)$ has also been used to evaluate the nature of the interactions in 2Imex1b-(*RS*), 2Imex**2**-(*RS*), and 2Imex3a-(*RS*) dimers. It is worth mentioning that the ratio $-G(r)/V(r)$ was introduced by Shianyan et al. (2010) for prediction of hydrogen bonds' nature. If the ratio $-G(r)/V(r)$ is > 1, then the interaction is purely non-covalent in nature (Shainyan et al. 2010). If the ratio falls between 0.5 and 1, the interaction is partly covalent. If the value is less than 0.5, the interaction is covalent in nature. As seen in Table 6, the $-G(r)/V(r)$ values are always between 0.5 and 1, indicating a partly covalent nature of the hydrogen bonds.

In the last column of Table 6, hydrogen bond energies calculated using the relationship $E_{HB} = V(r)/2$ described by (Espinosa et al. 1998) are listed. For the most stable dimer 2Imex**2**-(*RS*), the energy of NH····N interaction, according to Espinosa, is -8.88 kcal mol^{-1} (see Table 6). This value when compared with experimentally determined dissociation energy of the ammonia dimer (-2.8 kcal mol^{-1}) (Huisken and Pertsch 1988) gives an indication that the hydrogen bonding interaction of 2Imex**2**-(*RS*) is of medium strength. Notice the high value of E_{HB} obtained for 2Imex3a-(*RS*)

dimer, which is an indication of strong intermolecular hydrogen bond O–H····N (O_1H····N_2 and O_1H····N_2).

Free energy of association

To evaluate the direction in which the association process is evolving, the free energy association has been calculated in both gas and aqueous phases.

Free energy of association of the three dimers 2Imex**1b**-(*RS*), 2Imex**2**(*RS*), and 2Imex**3a**-(*RS*) was evaluated in both gas and water phases and the results are presented in Table 7 (more details on absolute free energies are listed on Table S6 of the Supporting Information).

Overall, the change of Gibbs free energy of association obtained in gas phase $\left(\Delta G^{\circ}_{ass}\right)$ at 298.15 K for imexon dimers 2Imex**1b**-(*RS*), 2Imex**2**-(*RS*), and 2Imex**3a**-(*RS*) was found to be negative, which suggests that these dimers can be spontaneously produced from the isolated monomers at room temperature in gas phase. However, in aqueous solution, Gibbs free energy $\left(\Delta G^{*}_{ass}\right)$ of dimerization obtained for the most stable dimers 2Imex**2**-(*RS*) and 2Imex**1b**-(*RS*) were found to be positive. This implies that association of the monomers will not occur spontaneously in aqueous solution.

In the case of 2Imex**3**-**a**-(*RS*) structure, our calculations suggest that this dimer is spontaneous in water; the calculated association free energy is clearly negative. For example the value $\Delta G^{\circ}_{ass} = -5.81$ kcal/mol has been obtained at M06-2X. This result is not unexpected because as shown before, the 2Imex**3**-**a**-(*RS*) dimer has stronger hydrogen bond interaction. The formation of 2Imex**3**-**a**-(*RS*) dimer is quite probable if favorable conditions are created for imexon tautomerization. However, it should be emphasized that at ambient temperature, the monomer that builds 2Imex**3a**-(*RS*), namely Imex**3**, is significantly less stable in aqueous phase (Kheffache et al. 2012, 2010), which makes improbable the formation of 2Imex**3a**-(*RS*) dimer in aqueous solution.

Results of this study suggest that, under normal conditions and low concentration, the antitumor drug imexon is not expected to form self-associated dimers in water solution.

Table 7 Free energies of association ΔG°_{ass} (kcal mol^{-1}) at 298 K in gas phase and standard state (1 M) free energies of association in the liquid phase ΔG^{*}_{ass} (kcal mol^{-1}) calculated at B3LYP/6-311+G(d,p) and M06-2X/6-311+G(d,p) levels and using SMD solvation model

Dimers	ΔG°_{ass}		ΔG^{*}_{ass}	
	B3LYP	M06-2X	B3LYP	M06-2X
2Imex1-b-(RS)	−2.64	−4.50	3.69	1.72
2Imex2-(RS)	−6.92	−8.95	6.20	4.00
2Imex3-a-(RS)	−12.28	−14.90	−3.27	−5.81

Conclusion

The main goal of the present study was to theoretically investigate the self-association of antitumor drug imexon. The thermodynamic stability and interaction energies of imexon dimers, resulting from self-association of the three imexon tautomers are investigated using B3LYP, M06-2X, and MP2 methods with 6-311++G(d,p) basis set. Among the dimers resulting from self-association of imexon tautomers, dimeric self-association of the oxo-amino tautomer is the most stable both in vacuum and in aqueous medium.

A theoretical study of the characteristics of the homo and heterochiral dimers of the three tautomers of imexon has also been carried out. Our results clearly show that the chiral discrimination process is very weak.

The analyses of the AIM and interaction energies have shown that all of the self-associated dimers, studied in this paper, satisfy the indicative criteria for hydrogen bonding interactions. The results of AIM analysis indicate that the OH····N intermolecular hydrogen bonds in 2Imex**3a**-(*RR*)/-(*RS*) are stronger than NH····N interactions of the most stable 2Imex**2**-(*RR*)/-(*RS*) dimers.

Finally, the free energy of association in aqueous phase was investigated using SMD solvation model. The results from the computational approach indicate that the most stable cyclic dimers 2Imex**2**-(*RR*)/-(*RS*) are found to be endergonic, non-spontaneous in aqueous solution.

References

Alkorta I, Zborowski K, Elguero J (2006a) Self-aggregation as a source of chiral discrimination. Chem Phys Lett. 427(4):289–294. https://doi.org/10.1016/j.cplett.2006.06.104

Alkorta I, Picazo O, Elguero J (2006b) Theoretical studies on chiral discrimination. Curr Org Chem 10(7):695–714. https://doi.org/10.2174/138527206776818955

Bader RFW (1985) Atoms in molecules. Acc Chem Res 18:9–15. https://doi.org/10.1021/ar00109a003

Becke AD (1993) Density-functional thermochemistry III. The role of exact exchange. J Chem Phys 98(7):5648–5652. https://doi.org/10.1063/1.464913

Boys SF, Bernardi F (1970) The calculation of small molecular interactions by the differences of separate total energies. Some procedures with reduced errors. Mol Phys 19(4):553–566. https://doi.org/10.1080/00268977000101561

Carroll MT, Bader RFW (1988) An analysis of the hydrogen bond in BASE-HF complexes using the theory of atoms in molecules. Mol Phys 65:695–722. https://doi.org/10.1080/00268978800101351

Den Brok MWJ, Nuijen B, Hillebrand MJX, Lutz C, Opitz H, Beijnen JH (2005) LC-UV Method development and validation for the investigational anticancer agent Imexon and identification of its degradation products. J Pharm Biomed Anal 38(4):686–694. https://doi.org/10.1016/j.jpba.2005.02.012

Espinosa E, Molins E, Lecomte C (1998) Hydrogen bond strengths revealed by topological analyses of experimentally observed

electron densities. Chem Phys Lett 285:170–173. https://doi.org/10.1016/S0009-2614(98)00036-0

Frisch MJ, Trucks GW, Schlegel HB, Scuseria GE, Robb MA, Cheeseman JR, Scalmani G, Barone V, Petersson GA, Nakatsuji H, Li X, Caricato M, Marenich AV, Bloino J, Janesko BG, Gomperts R, Mennucci B, Hratchian HP, Ortiz JV, Izmaylov AF, Sonnenberg JL, Williams-Young D, Ding F, Lipparini F, Egidi F, Goings J, Peng B, Petrone A, Henderson T, Ranasinghe D, Zakrzewski VG, Gao J, Rega N, Zheng G, Liang W, Hada M, Ehara M, Toyota K, Fukuda R, Hasegawa J, Ishida M, Nakajima T, Honda Y, Kitao O, Nakai H, Vreven T, Throssell K, Montgomery JA, Jr, Peralta JE, Ogliaro F, Bearpark MJ, Heyd JJ, Brothers EN, Kudin KN, Staroverov VN, Keith TA, Kobayashi R, Normand J, Raghavachari K, Rendell AP, Burant JC, Iyengar SS, Tomasi J, Cossi M, Millam JM, Klene M, Adamo C, Cammi R, Ochterski JW, Martin RL, Morokuma K, Farkas O, Foresman JB, Fox DJ (2016) Gaussian 16, Revision A.03, Gaussian, Inc., Wallingford CT

Huisken F, Pertsch T (1988) Infrared photodissociation of size-selected small ammonia clusters. Chem Phys 126(1):215–228. https://doi.org/10.1016/0301-0104(88)85034-1

Kheffache D, Ouamerali O (2010) What is the real existing form of imexon? Quantum chemical studies. J Mol Struct THEOCHEM 945(1):39–44. https://doi.org/10.1016/j.theochem.2010.01.010

Kheffache D, Guemmour H, Ouamerali O (2012) Prototropic tautomerism and microsolvation in antitumor drug imexon: a DFT study. Struct Chem 23(5):1547–1557. https://doi.org/10.1007/s11224-012-9968-3

Koch U, Popelier PLA (1995) Characterization of C–H–O hydrogen bonds on the basis of the charge density. J Phys Chem 99:9747–9754. https://doi.org/10.1021/j100024a016

Kuehl PJ, Carducci MD, Myrdal PB (2006) 4-Imino-1,3-diaza-bicyclo-[3.1.0]hexan-2-one. Acta Crystallogr Sect E 62:o3688–o3690. https://doi.org/10.1107/S1600536806029412

Lee C, Yang W, Parr RG (1988) Development of the Colle-Salvetti correlation-energy formula into a functional of the electron density. Phys Rev B 37:785–789. https://doi.org/10.1103/PhysRevB.37.785

Lu T, Chen F (2012) Multiwfn: a multifunctional wavefunction analyzer. J Comput Chem 33:580–592. https://doi.org/10.1002/jcc.22885

Marenich AV, Cramer CJ, Truhlar DG (2009) Universal solvation model based on solute electron density and on a continuum model of the solvent defined by the bulk dielectric constant and atomic surface tensions. J Phys Chem B 113(18):6378–6396. https://doi.org/10.1021/jp810292n

Matta CF, Boyd RJ (2007) In the quantum theory of atoms in molecules: from solid state to DNA and drug design. Wiley, Weinheim

Møller C, Plesset MS (1934) Note on an Approximation treatment for many-electron systems. Phys Rev 46:618–622. https://doi.org/10.1103/PhysRev.46.618

Moulder S, Dhillon N, Ng C, Hong D, Wheler J, Naing A, Tse S, La Paglia A, Dorr R, Hersh E, Boytim M, Kurzrock R (2010) A phase I trial of imexon, a pro-oxidant, in combination with docetaxel for the treatment of patients with advanced breast, non-small cell lung and prostate cancer. Invest New Drugs 28(5):634–640. https://doi.org/10.1007/s10637-009-9273-1

Popelier PLA (1998) Characterization of a Dihydrogen bond on the basis of the electron density. J Phys Chem A 102:873–1878. https://doi.org/10.1021/jp9805048

Remers WA, Dorr R (2012) Chemistry and pharmacology of Imexon and related Cyanoaziridines. Curr Med Chem 19(33):5745–5753. https://doi.org/10.2174/092986712803988802

Ribeiro RF, Marenich AV, Cramer CJ, Truhlar DG (2011) The solvation, partitioning, hydrogen bonding, and dimerization of nucleotide bases: a multifaceted challenge for quantum chemistry. Phys Chem Chem Phys 13(23):10908–10922. https://doi.org/10.1039/c0cp02784g

Rode JE, Dobrowolski JC (2002) Theoretical studies on the oxetane··· HCl and thietane··· HCl complexes. Chem Phys Lett 360(1–2):123–132. https://doi.org/10.1016/S0009-2614(02)00779-0

Rode JE, Jamróz MH, Dobrowolski JC, Sadlej J (2012) On vibrational circular cichroism chirality transfer in electron donor-acceptor Complexes: a Prediction for the Quinine···BF3 system. J Phys Chem A 116(30):7916–7926. https://doi.org/10.1021/jp304955v

Shainyan BA, Chipanina NN, Aksamentova TN, Oznobikhina LP, Rosentsveig GN, Rosentsveig IB (2010) Intramolecular hydrogen bonds in the sulfonamide derivatives of oxamide, dithiooxamide, and biuret. FT-IR and DFT study, AIM and NBO analysis. Tetrahedron 66(44):8551–8556. https://doi.org/10.1016/j.tetlet.2010.08.076

Sheveleva EV, Landowski TH, Samulitis BK, Bartholomeusz G, Powis G, Dorr RT (2012) Imexon induces an oxidative endoplasmic reticulum stress response in pancreatic cancer cells. Mol Cancer Res 10(3):392–400. https://doi.org/10.1158/1541-7786.MCR-11-0359

Zhao Y, Truhlar DG (2008) The M06 suite of density functionals for main group thermochemistry, thermochemical kinetics, noncovalent interactions, excited states, and transition elements: two new functionals and systematic testing of four M06-class functionals and 12 other functionals. Theor Chem Acc 120:215–241. https://doi.org/10.1007/s00214-007-0310-x